Discrimination Between Hypogene and Supergene Sulfates: Questa Mine Site, Taos County, New Mexico

by

Shubha Pandey
MS Project Report
Advisor: Andrew Campbell
Department of Geochemistry
New Mexico Tech, Socorro, NM
Spring 2004

New Mexico Tech
SCIENCE · ENGINEERING · RESEARCH · UNIVERSITY

Abstract

The Questa molybdenum mine is located in Taos county, north-central New Mexico. The mine site consists of an open pit, various rock piles, and several naturally occurring alteration scars. The waste rock piles in the Questa area are situated on steep slopes in the Red River drainage. Due to the high angle of repose, long-term geotechnical stability of these piles is of major concern. The waste rocks contain a significant concentration (1-5 wt %) of sulfide minerals, mainly pyrite. Because these minerals oxidize readily, the chemical and mineralogical changes due to the weathering are of particular concern in their long-term stability. In order to quantify the weathering related mineralogical changes in the pile the supergene versus hypogene mineral origins need to be determined. Stable isotope analysis on sulfates such as, jarosite [$KFe_3(SO_4)_2(OH)_6$], alunite [$KAl_3 (SO_4)_2(OH)_6$], and gypsum [$CaSO_4.2H_2O$] is a very useful tool in differentiating hypogene versus supergene origin of these sulfates. In addition, naturally occurring alteration scars can provide an analogy of the mineralogical changes that can occur in the waste piles with time.

The $\delta^{34}S$ values obtained from gypsum show a large variation from deeper levels to near surface environment. In deeper levels, $\delta^{34}S$ of gypsum ranges from +6 ‰ to +9 ‰ (magmatic), while at shallower levels the values are close to +12.1 ‰ and the values near surface ranges from −0.1 to −0.71 ‰ (supergene). The $\delta^{34}S$ of gypsums from waste rock piles gave two ranges of values: one towards the heavier (8.2 to 11.2 ‰), and the rest towards lighter between the range of 0.9 to 2.6 ‰. These two ranges of $\delta^{34}S$ suggest that there was already some sulfate of primary origin present at the time of dumping these waste piles.

The fluid composition calculated from hydrogen and oxygen isotope data from jarosite reflects meteoric water. The $\delta^{34}S$ values of jarosite (range from −0.15 to −4.35 ‰) are found to be in close proximity to that of pyrite (~0 ‰). This reflects jarosite formation from the oxidation of pyrite in the weathering environment. When plotted, $\delta^{18}O$ and δD values fall nicely into the supergene jarosite field with δD values showing some elevation dependence ranging from −140 to −178 ‰.

The $\delta^{34}S$ obtained for alunite (~17.0 ‰) is significantly different than that for jarosite indicating magmatic influence in the former. The $\delta^{18}O$ and δD of alunite further support this assumption (these values fall outside of the supergene alunite fields). The fluid composition calculated from hydrogen and oxygen isotope data of alunite reflects meteoric water source. A possible explanation for this may be as follows. The alunite formation by magmatic vapors containing H_2S migrated upward through the fractures and condensed into the meteoric water, which reacted to form H_2SO_4. This H_2SO_4 further reacted with feldspar in the andesite and formed alunite.

Table of Content

1. Introduction.

Questa is a molybdenum mine located in north-central New Mexico. The mine site has several waste rock piles with high slope angles that resulted from open pit mine activities. Due to steep slopes of these piles, long-term stability of these piles is a major concern. Waste rock piles in the Questa area contain significant amount of sulfide minerals (principally pyrite) that are prone to rapid weathering. Therefore, an understanding of the mineralogical and geochemical changes in the waste piles with time due to weathering will be very helpful in assessing the stability of these piles. However, in judging the extent of pile weathering, naturally occurring alteration scars in the Questa area can provide an analogy of the mineralogical changes that can occur in the waste piles with time. Recognition of the minerals that were already present at the time of dumping the piles (i.e., hypogene + supergene) versus the minerals that are being formed today in the piles due to weathering is necessary.

Stable isotopes of sulfate minerals (jarosite, alunite, and gypsum) are useful in providing information about the origin of these minerals (Rye and Stoffregen, 1995). These sulfates can be formed either in the hypogene or the supergene environment (Rye and Alpers, 1997).

Jarosite $[KFe_3(SO_4)_2(OH)_6]$ and isostructural alunite $[KAl_3(SO_4)_2(OH)_6]$ contain both hydroxyl and sulfate sites. Therefore, stable isotopic analysis can be performed on all four isotopic sites; sulfur, hydrogen, oxygen in sulfate, and oxygen in hydroxyl group. Stable isotopic study of all the isotopes together will give information about the origin of these sulfates (based upon Wasserman et al, 1992 and Stoffregen et al, 1994).

4

2. Background and Geological History.

The Molycorp Questa molybdenum mine is located on the western slope of the Taos range of the Sangre de Cristo mountains in north-central New Mexico (Briggs et al, 2003 and Meyer et al, 1990). The mine property lies north of NM Highway 38 between the towns of Questa and Red River. The site contains an open pit, several waste rock piles and alteration scars.

The mine site is an area of complex geological history; located in a faulted zone that is several miles wide and trends eastward (Ross et al, 2002). The relief of the area is steep, ranging from 2400 meter on the Red River to over 2900 meter at higher elevations.

Precambrian metamorphic rocks form the basement rock in the area. Basement rocks are overlaid by a sequence of Tertiary andesitic volcanic rocks, rhyolitic tuff, basalt megabreccias followed by a late Oligocene Latir volcanic field volcanism (Meyer et al, 1990). Latir volcanism resulted in the formation of the Questa Caldera that was the source of the Amalia tuff. The collapse of the Caldera and associated ring fracturing as well as the crustal extension are related to the formation of Rio Grande rift zone (Figure 1). Crustal extension resulted in a 90˚ westward tilting of the entire Southern Caldera region. Brecciation along with the low angle fault zones is observed throughout the Questa Red River region. Hydrothermal fluids circulated within these fracture zones resulted in molybdenum mineralization and pyritization of these areas. Beside mineralization, these fracture zones also acted as zones of weaknesses for future land sliding and scar formation (Meyer et al, 1990).

Hydrothermal activity in the mine area was generated primarily due to the intrusion of several plutons during Tertiary volcanism and is responsible for much of the

hydrothermal alteration of the surrounding rocks. The hydrothermally altered rocks typically contain chloride, epidote, quartz, carbonates, sericite, and clay minerals. Due to the Late Miocene to present rifting, Sangre de Cristo Mountains are uplifted along high angle normal faults at the eastern margin of the modern rift basin, which further exposed the Latir Volcanic field and hydrothermally altered zones (Ross et al, 2002).

There are around twenty alteration scars present in the Questa area (in the vicinity of the pit as well as beneath some of the mine waste rock piles). These alteration scars are formed due to the weathering of the hydrothermally altered rocks (with high pyrite content; >3% pyrite). Most of the scars are located north of the Red River, on and off the mine site, and east of the town of Red River (Figure 2). These scars are typically characterized by yellow-stained and easily eroded material that supports almost no vegetation.

3. Experimental.

Sample Description

Representative samples were collected of different sulfides and sulfates from the ore body, alteration scars, and rock piles.

The ore body samples of sulfides, anhydrite, gypsum (both from ore body and above the ore body) and possibly alunite should be the representative of hypogene minerals. Alteration scars in the area are formed due to the long term weathering of the hydrothermally altered volcanic rocks. Therefore, they should contain supergene minerals such as, jarosite, gypsum, and alunite. The waste piles in the Questa mine area

6

are currently undergoing the weathering process. Due to the weathering, we should be able to find more supergene jarosite and gypsum that formed subsequent to dumping.

Sample Collection.

The samples of different sulfates, e.g., jarosite, $[KFe_3(SO_4)_2(OH)_6]$, alunite $[KAl_3(SO_4)_2(OH)_2]$, gypsum $[CaSO_4.2H_2O]$, etc. were collected from different locations of Questa mine area. Further, some drill core samples of gypsum, anhydrite and pyrite are obtained from ore body and just above the ore body. Around twelve rock samples containing jarosite and gypsum were collected from the following sites: Sugar Shack South waste pile, Sugar Shack waste pile, and Sulfur Gulch South waste pile. Six alteration scar samples containing gypsum, alunite, and jarosite were collected from the following sites: Pit scar, Hottentot scar, Hanson scar, Straight Creek South and East, Bitter Creek scar, and Capulin scar. A complete detail of all the samples and their locations are provided in Table 1.

Sample Preparation.

Pure jarosite, alunite, and gypsum were obtained from rock samples by appropriate and careful handpicking. X-ray diffraction is used to assess their purity. Due to the coarse nature of the grains of gypsum and jarosite not much cleaning was required except for some washing with de-ionized water followed by drying. In alunite samples, however, kaolinite and clay are more troublesome impurities, but can be removed by applying several steps of shaking and ultrasonication followed by dissolution with hydrofluoric acid. Further details of this procedure can be found in Appendix 1. In the end, samples were powdered to avoid any inhomogeneities.

Chemical Separation.

In all of the sulfate samples, oxygen is present in two sites: sulfate (O in SO_4) and in

hydroxyl (O in OH or H_2O) [e.g., alunite: $KAl_3(SO_4)_2(OH)_2$, jarosite: $KFe_3(SO_4)_2(OH)_6$,

and gypsum: $CaSO_4.2H_2O$]. In order to perform $\delta^{18}O$ analysis on both sites, we have to

separate oxygen in SO_4 site from that in OH site. All SO_4 in the sample is selectively

separated as $BaSO_4$ by initially dissolving the sample in a heated solution of 0.5 N NaOH

followed by titration with 10 N HCl and addition of $BaCl_2$ (Wasserman et al, 1992). Step

by step procedure for this separation process is provided in Appendix 1.

Method.

<u>Isotopic Analysis</u>. Isotopic analysis on jarosite, alunite, gypsum and anhydrite ($CaSO_4$)

were performed on a Thermo Finnigan Delta Plus XP Continuous Flow Isotope Ratio

Mass Spectrometer (CFIRMS). Sample sizes for different minerals for different isotopic

analysis are given in Appendix 2.

(1) *Sulfur in sulfate sites ($\delta^{34}S$)*. $\delta^{34}S$ analysis of jarosite, alunite, gypsum, anhydrite, and

selected pyrite are carried out using an Elemental Analyzer (EA) interfaced with

CFIRMS. Each dried sample was weighted on an analytical microbalance in small tin

cups (dimensions: 3.5×5.0 mm). Different sample weights were used for different

samples depending on their sulfur contents relative to 400-µg of the reference

material. The details of different weights used for different sulfates, sulfides, and

standards are provided in Appendix.

Standard materials, such as NBS sphalerite, NBS Ag_2S, NBS 127 $BaSO_4$ and in-

house standard FeS are weighed with each set of samples - in the beginning, in the

end, and in between the set of samples to maintain the quality standard protocol. In

8

each batch some samples were run in duplicate. Samples are loaded into the EA auto-sampler and all the information regarding the sample (e.g., sample ID, weight, etc.) is entered into the ISODAT program on the computer that subsequently controls CFIRMS. Each run on the mass spectrometer results in an initial sample peak followed by three reference peaks; the complete analysis takes ~12-15 minutes. After each set of run, $\delta^{34}S$ values obtained from the instrument are corrected for sample size (size correction equation is obtained by running standard materials at different sample sizes) and by correction equation obtained after plotting measured versus known (or given) $\delta^{34}S$ of the standards (relevant data for standards is provided in Appendix 2). V_2O_5 is added to all sulfate samples to achieve better combustion.

(2) *Hydrogen (δD).* δD analysis of jarosite, gypsum, and alunite are performed with a TCEA interfaced with CFIRMS. The analysis is performed in the same way as that for $\delta^{34}S$ on EA, except that silver cups are used instead of tin cups. Standard materials that are used with each sample batch are polyethylene and HEKA benzoic acid. After each analysis δD are corrected by linear regression analysis obtained on measured versus actual δD of standards. No size correction was performed on δD values.

(3) *Oxygen in sulfate and hydroxyl sites ($\delta^{18}O_{SO4}$ and $\delta^{18}O_{OH}$).* $\delta^{18}O_{SO4}$ are obtained by analyzing $BaSO_4$ obtained from different samples (*vide supra*) using TCEA interfaced with CFIRMS. Standards NBS 127 $BaSO_4$ and HEKA benzoic acid were run with each batch of samples. $\delta^{18}O_{OH}$ were obtained by first analyzing the total bulk oxygen isotopic composition followed by utilizing already obtained $\delta^{18}O_{SO4}$

along with the corresponding mole fractions of oxygen in both sites calculated from stoichiometrically correct mineral chemical formulae.

(4) *Isotopic composition of water.* Isotopic composition of fluids responsible for the formation of gypsum, alunite and jarosite are calculated based upon the fractionation factors obtained in the following references: Rye and Stoffregen, 1995, Stoffregren et al, 1994, and Seal, 2003. Fractionation equations are given in Appendix 3.

4. Results.

 The isotopic values for all four isotopes as well as the calculated fluid compositions for the samples of gypsum, alunite, jarosite, anhydrite and pyrite are tabulated in Table 2.

$\delta^{34}S$ values.

 $\delta^{34}S$ obtained for whole rock and ore body pyrites are ~3.0 ‰ and 1.0 to 2.5 ‰, respectively.

Gypsum. Gypsum $\delta^{34}S$ just above the ore body is 12.3 ‰ and that from ore body ranges from 12.6 to 8.0 ‰. On the other hand, $\delta^{34}S$ from ore body anhydrite ranges from 6.6 to 10.0 ‰. Gypsum from waste piles shows a large range of $\delta^{34}S$, some closer to those of the gypsum in ore body (between 8.2 to 11.2 ‰), while others closer to the jarosite and pyrite $\delta^{34}S$ (between 0.9 to 2.6 ‰). One gypsum sample from alteration scar gave $\delta^{34}S$ close to 0.43 ‰, which is again close to the jarosite and pyrite $\delta^{34}S$. The distribution of the $\delta^{34}S$ is effectively depicted using in Figure 3 and 4.

Jarosite.   Jarosite $\delta^{34}S$ obtained from the alteration scars are in the range of −6.5 to 0.15 ‰. Interestingly, one jarosite from waste pile gave a $\delta^{34}S$ of 2.2 ‰.

<u>Alunite</u>. Alunite from alteration scar in Amalia Tuff has $\delta^{34}S$ of 17.5 ‰, which is significantly higher.

$\delta^{34}S$ obtained for gypsum, anhydrite and pyrite from ore body reflect their possible origin in magmatic environment. The higher $\delta^{34}S$ of the gypsum from just above the ore body can be explained on the basis of higher fractionation due to lower temperature than ore body. $\delta^{34}S$ of pyrite (1.0 to 3.0 ‰) can be used as a reference point to discriminate the sulfates to see whether they have formed by the weathering of the pyrite. If the sulfates are formed by the weathering, their sulfur values should be closer to those of the precursor pyrite (Rye, 1997).

$\delta^{18}O_{SO4}$.

<u>Gypsum</u> $\delta^{18}O_{SO4}$ of gypsum and anhydrite from ore body are in the range of 5.0 to 9.4 ‰, which is toward the heavier side. $\delta^{18}O_{SO4}$ of gypsum from waste piles show two ranges. One toward heavier $\delta^{18}O_{SO4}$ (in the range of 5.3 to 8.7 ‰), similar to that of alunite and ore body gypsum, while the other toward the lighter values, in the range of – 6.0 to −1.89 ‰, closer to jarosite $\delta^{18}O_{SO4}$. One of the gypsum samples from waste rock pile gave a very depleted $\delta^{18}O_{SO4}$ value of −9.33 ‰ (figure 4).

<u>Alunite</u> $\delta^{18}O_{SO4}$ of alunite also shows a heavier value (7.5 ‰).

<u>Jarosite</u> jarosites gave relatively lighter (in the range of 2.2 to −3.3 ‰).

$\delta^{18}O_{OH}$.

<u>Gypsum</u> $\delta^{18}O_{OH}$ of gypsum samples from ore body and just above the ore body are in the range of −4.7 to −12.8 ‰. Some of the gypsum samples from the waste rock piles (e.g., the ones with higher $\delta^{34}S$ and $\delta^{18}O_{SO4}$) have $\delta^{18}O_{OH}$ from −24.1 to −13.5 ‰, except for the one that has a less negative value −5.26 ‰. Rest of the gypsum samples from waste

rock piles and alteration scars (e.g., the ones with lower $\delta^{34}S$) gave $\delta^{18}O_{OH}$ in the range –14.3 to –9.36 ‰, again with one exception (–23.9 ‰).

Alunite Alunite $\delta^{18}O_{OH}$ is –2.05 ‰.

Jarosite All jarosite $\delta^{18}O_{OH}$ are in the range of –6.8 to –2.03 ‰.

$\delta D.$

 Gypsum δD of gypsum from the ore body and close to the ore body are between –123 to –115 ‰. Gypsum samples from alteration scars as well as those from waste rock piles gave δD in the range of –92.5 to –122.8 ‰, except for one that has very depleted δD (–204 ‰).

 Alunite Alunite has δD –47 ‰.

Jarosite Jarosite has δD –178 to –140 ‰, except for one jarosite from waste pile with a δD of –106 ‰.

5. Discussion.

Gypsum. Most of the gypsums from different locations have δD values that fall between the δD values of jarosite and alunite (refer to Figure 5). This can be attributed to the formation of gypsum at different periods than those for jarosites and alunite. One δD value of gypsum from waste rock pile shows a very depleted value, which is hard to explain at this time.

$\delta^{18}O_{OH}$ show a wide range from –24.1 to – 4.7 ‰ in comparison to $\delta^{18}O_{SO4}$, which lie in a rather narrow range (–6.0 to 9.4 ‰). The $\delta^{18}O_{SO4}$ for all the gypsums obtained from the ore body, one just above the ore body, and the few from the waste piles form a cluster and locate themselves toward the heavier values of $\delta^{18}O_{SO4}$ (Figure 6 & 7).

It is important to mention that these gypsum samples also show higher $\delta^{34}S$ values (Figure 4). A very different pattern has been observed for the rest of the gypsum samples that are collected from alteration scar and waste piles. These gypsum samples have low $\delta^{34}S$ values (close to those of pyrite); they fall toward the low $\delta^{18}O_{SO4}$ values, and when plotted together with jarosite and alunite, they fall very close to the jarosite values but far from the alunite values (Figure 5).

From the above observations we can suggest that gypsum isotopic values show two types of origin – the first from the ore body that may indicate that some of the gypsum in the waste piles are hypogene in nature, while the second from the alteration scars that renders the rest of the waste piles to be supergene in nature. The calculated fluid compositions of the gypsum samples do not provide any further useful information; these values are scattered.

Jarosite. δD versus $\delta^{18}O$ for jarosite alone from different locations is shown in Figure 8. All $\delta^{18}O_{OH}$ and $\delta^{18}O_{SO4}$ fall nicely within the supergene jarosite fields except for one value (from the waste pile). The calculated isotopic composition of the fluid from the jarosite OH site lies very close to the meteoric water line except for one value from the waste pile that falls a little further from the meteoric water line (supergene jarosite and alunite fields are obtained from the work of Rye, 1997). It is important to mention that similar patterns for the supergene jarosites are observed in the mine data from different mines by Rye, 1997. The δD values of jarosite from different elevations show a range that can be explained on the basis of climatic changes in the past. The supergene origin of the jarosite is further supported by their $\delta^{34}S$ values (−4.35 to 0.15 ‰) that are very

close to the $\delta^{34}S$ of their precursor pyrite (1.0 to 3.0 ‰). This clearly links the formation of these jarosites to the weathering of pyrite.

Alunite. $\delta^{18}O_{SO4}$ and $\delta^{18}O_{OH}$ from alunite are very different than those from jarosite (see Figure 5). The $\delta^{18}O$ values from both hydroxyl and sulfate sites for alunite do not convincingly fall in the appropriate alunite supergene fields, reflecting the possible absence of the influence of weathering environment on their formation. It is important to mention that the calculated fluid composition for alunite falls right on the meteoric water line. Further, the $\delta^{34}S$ of alunite is fairly high (17.8 ‰) and significantly different from those of pyrite and supergene jarosites (Figure 4). The high $\delta^{34}S$ value of alunite requires derivation of sulfur from magmatic SO_2, which may have escaped from magma through fractures and subsequently condensed into the meteoric water. A further interaction of the sulfur in the meteoric water with the feldspar in the volcanic rocks may have formed this alunite. A similar kind of alunite has been reported in an investigation by Rye et al, 1997. They called this type of alunite as magmatic hydrothermal alunite.

The δD value (–47.0 ‰) of the alunite is very different than that of jarosite due to the small fractionation factor between alunite and water.

6. Conclusion.

Based on our overall results we can suggest that the stable isotope analysis of sulfates is definitely a reliable and efficient method to investigate and explore the origins of acid sulfates. All the jarosites in our study indicate that their formation is due to the weathering of the pyrite in the volcanic rocks. On the other hand, alunite is magmatic hydrothermal. This can be explained by the movement of the magmatic SO_2 through fractures followed by the condensation in the ground water, which further reacted to form

H_2SO_4 and subsequently formed alunite by reacting with the feldspar in the rocks. Gypsums, on the basis of their $\delta^{18}O_{SO4}$ and $\delta^{34}S$, show both hypogene and supergene origins. Based on the fact that the origin of gypsums obtained from the waste piles is both hypogene and supergene in nature, we can conclude that the pyrite in the weathering piles is not responsible for the formation of acid sulfates in the piles, and that some of the sulfates were already present at the time of the dumping of these piles.

7. References.

1) Briggs, P.H., Sutley, S.J., and Livo, K.E. 2003. Questa baseline and pre-mining ground water investigation: 11. Geochemistry of composited material from alteration scars and mine-waste piles, U.S. Geological Survey, Open-file Report 03-458.

2) Meyer, J., and Leonardson, R. 1990. Tectonic, hydrothermal and geomorphic controls on alteration scars formation near Questa, New Mexico, New Mexico Geological Society Guidebook, 41st Field Conference, Southern Sangre de Cristo Mountains, New Mexico, p. 417-422.

3) Ross, P.S., Jébrak, M., and Walker, B.M. 2002. Discharge of the hydrothermal fluids from a magma chamber and concomitant formation of a stratified breccia zone at the Questa porphyry molybdenum deposit, New Mexico, Economic Geology, v. 97, p. 1679-1699.

4) Rye, R.O., and Stoffregen, R.E. 1995. Jarosite-water oxygen and hydrogen fractionations: Preliminary experimental data, Economic Geology, v. 90, p. 2336-2342.

5) Rye, R.O., and Alpers, C.N. 1997. The stable isotope geochemistry of jarosite, U.S. Geological Survey, Open-file Report 97-88.

6) Seal, R.R. II. 2003 in Environmental Aspects of Mine Waters, Mineralogical Association of Canada, Short Course series, vol 31, Jambor, J.L., Blowes, D.W., Ritchie, A.I.M (editors), Raeside, R. (series editor), Vancouver, British Columbia, Chapter 5.

7) Stoffregen, R.E. et al 1994. Experimental studies of alunite: I. ^{18}O- ^{16}O and D-H fractionation factors between alunite and water at 250-450 ˚C, Geochimica et Cosmochimica Acta, v. 58, p. 903-916.

8) Wasserman, M.D. et al 1992. Methods for separation and total stable isotope analysis of alunite, U.S. Geological Survey, Open-file Report 92-9.

8. Tables

Table 1. Samples and their locations.

Sample ID	Mineral	Location
SSS VWL 0001	Gypsum	Sugar Shack South Waste Pile, around Breather block
SSS VWL 0002	Gypsum & Jarosite	Sugar Shack South Waste Pile, around Breather
SSS VWL 0003	Gypsum	Large gypsum crystals sitting on top of the bench
SSW VWL 0001	Gypsum	Sugar Shack West waste Pile, from clay rich layer
SSW VWL 0002	Gypsum	Selenite crystals with jarosite
SSW VWL 0003	Gypsum	Fine needles of gypsum in mud
SGS VWL 0001	Gypsum	Sulfur Gulch South Waste Pile, fractures in black andesite
SGS VWL 0002	Gypsum	Gypsum in mud
SGS VWL 0003	Gypsum	Fractured pit Porphyry with abundant gypsum-moly
SGS VWL 0004	Gypsum	Fractured andesite, around cold Breather Hole
SGS VWL 0005	Gypsum	Anhydrite conversion to gypsum, flourite also present
PIT VWL 0007	Jarosite	Pit Scar, NW edge, altered vein filled with alunite and jarosite in Amelia tuff
HTS USG 0005 07	Alunite	Hottentot Scar, From Amelia tuff
SWH VWL 0001 07	<u>Jarosite</u>	Hanson Scar, large Ferricrete
ESS VWL 0001 07	Jarosite	East of Straight Creek Scar, vein in altered volcanics
BCS VWL 0002 07	Jarosite	Bitter Creek Scar
CAS VWL 0007 07	Jarosite	Capulin Scar, jarosite /hematite from large Ferricrete
GMG PIT 0001	Gypsum	Gypsum from just above the ore body
SCS VWL 0005	Gypsum	Straight Creek South Scar, gypsum flowers

Some of the gypsum and anhydrite samples not listed here are drill core samples from the ore body.

Sample ID	Mineral	δ^{34}S	δD (OH)	δ^{18}O (SO$_4$)	δ^{18}O (bulk)	δ^{18}O (OH)	δD (H$_2$O)	δ^{18}O (H$_2$O) OH	δ^{18}O (H$_2$O) SO4	$\Delta_{(SO4-OH)}$	T (ºC)
AR 163	Anhydrite	7.97		3.50							
AR 89	Anhydrite	9.58		5.37							
AR 165	Anhydrite	6.63		7.34							
AR-23	Gypsum	12.6	-122.9	9.40	4.04	-8.47	-107.0	-12.2			
AR-140	Gypsum	9.98	-117.4	5.90	2.60	-5.10	-102.0	-8.80			
AR-165	Gypsum	9.85	-114.7	6.70	2.60	-7.00	-99.70	-10.7			
AR-86	Gypsum	8.00	-114.0	6.00	0.37	-12.8	-99.00	-16.5			
GMG PIT 0001 07	Gypsum	12.3	-114.9	5.00	-1.15	-4.70	-99.90	-8.40			
SSS VWL 0002 07	Gypsum	2.60	-104.7	-4.70	-6.07	-9.36	-89.70	-13.1			
SSW VWL 0002 07	Gypsum	2.45	-104.6	-3.65	-6.69	-13.7	-89.60	-17.4			
SSW VWL 0003 07	Gypsum	2.15	-115.3	-6.00	-7.40	-10.7	-100.0	-14.4			
SGS VWL 0002 07	Gypsum	0.90	-201.4	-9.33	-13.7	-23.9	-186.4	-27.6			
SGS VWL 0001 07	Gypsum	10.8	-121.9	4.19	-2.33	-5.26	-106.9	-9.00			
SSSVWL 0003 07	Gypsum	11.2	-120.7	5.30	-0.35	-13.5	-105.0	-17.2			
SGS VWL 0003 07	Gypsum	8.74	-107.1	6.20	-2.70	-24.1	-92.10	-27.8			
SGS VWL 0004 07	Gypsum	9.95	-116.9	6.20	-2.01	-21.2	-101.9	-24.9			
SGS VWL 0005 07	Gypsum	8.81	-92.50	8.70	0.27	-19.4	-77.50	-23.1			
SCS VWL 0005 07	Gypsum	0.43	-122.8	-1.89	-5.62	-14.3	-107.8	-18.0			
SSS VWL 0002 07	Jarosite	2.16	-105.9	-3.30	-4.50	-6.30	-55.00	-19.0	-32.42	3.00	847
PIT VWL 0007 07	Jarosite	-6.50	-154.99	-0.96	-3.30	-6.80	-105.0	-19.5	-30.10	5.80	326
HTS USG 0005 07	Alunite	17.8	-47.00	7.50	3.40	-2.05	-41.00	-6.50	-0.840	9.60	32.2
BCS VWL 0002 07	Jarosite	-0.15	-177.5	2.20	-0.60	-3.04	-127.5	-16.0	-26.92	5.24	377
CAS VWL 0007 07	Jarosite	-0.17	-175.0	0.40	-1.70	-4.48	-125.0	-17.1	-28.70	4.90	415
ESS VWL 0001 07	Jarosite	-1.30	-140.0	2.70	-0.10	-3.35	-90.00	-16.1	-26.40	6.10	311
SWH VWL 0001 07	Jarosite	-4.35	-163.0	-1.80	-1.90	-2.03	-113.0	-14.6	-30.92	0.23	-

- All δ values are in ‰ and are averaged over all the duplicate measurements as well as re-runs.
- Fractionation equation to calculate the fluid composition for jarosite, alunite, and gypsum are given in Appendix.
- δ^{34}S values for pyrite and are not included above; they are as follows:
  Pyrite (ore body)   1.0 to 2.5‰
  Pyrite (whole rock)   ~3 ‰
- δ^{34}S values of anhydrite and pre body pyrite are taken from a MS thesis (work in progress) of Amanda Rowe (graduate student in Geology)

Table 2. Samples and their δ values for oxygen, hydrogen, and sulfur.

9. Figures

Figures 1, and 2 are not here (need to scan them).
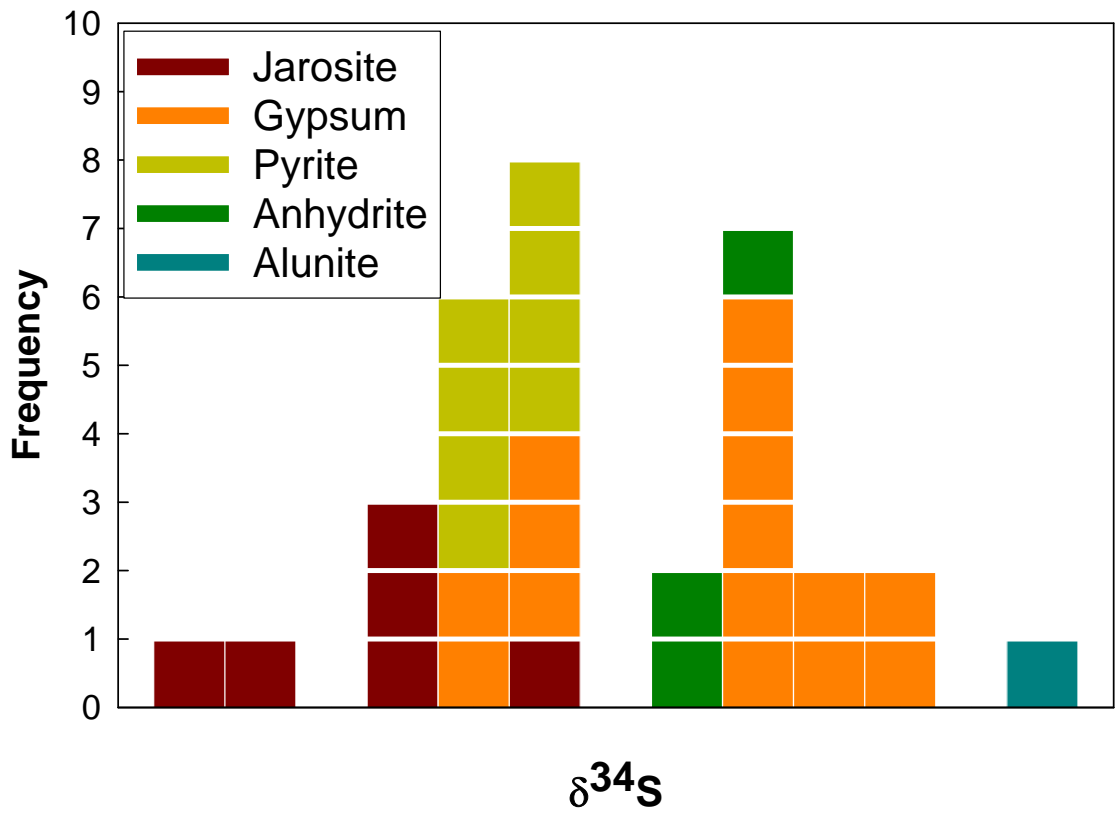
Figure 3. Histrogram showing distribution of $\delta^{34}S$ values for jarosite, alunite, gypsum, pyrite, and anhydrite from different locations.
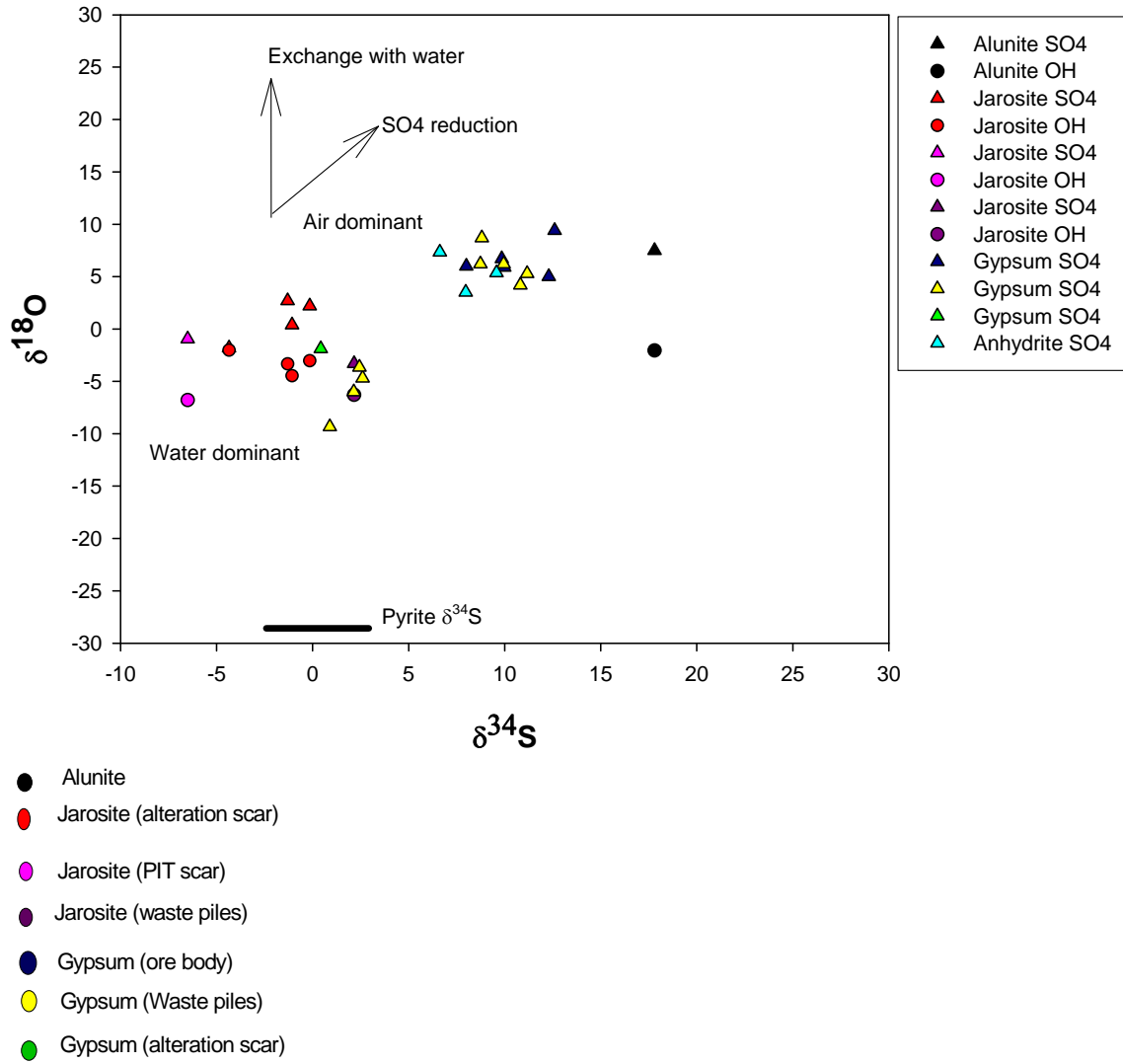
Figure 4. Plot between δ 18O vs. δ 34S of different minerals from different locations.
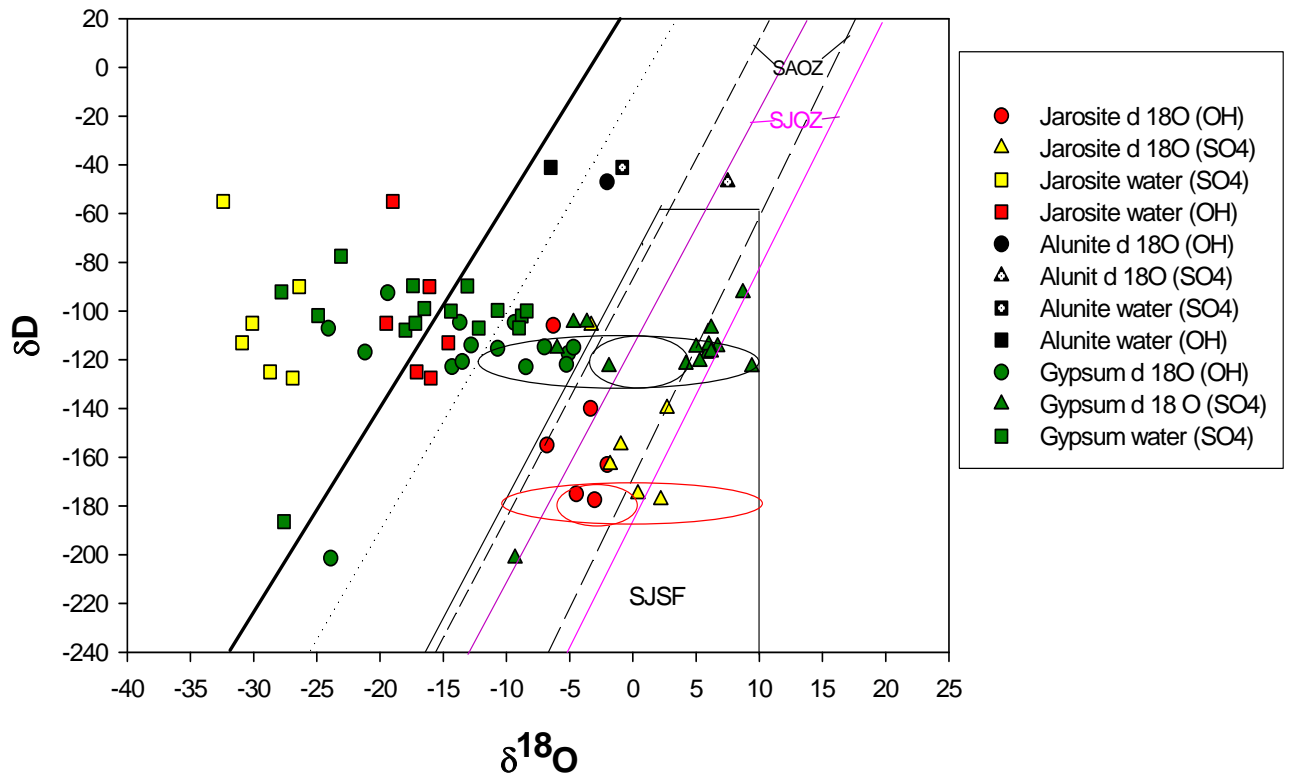
Figure 5. Graph of δD vs. δ¹⁸O for different minerals.
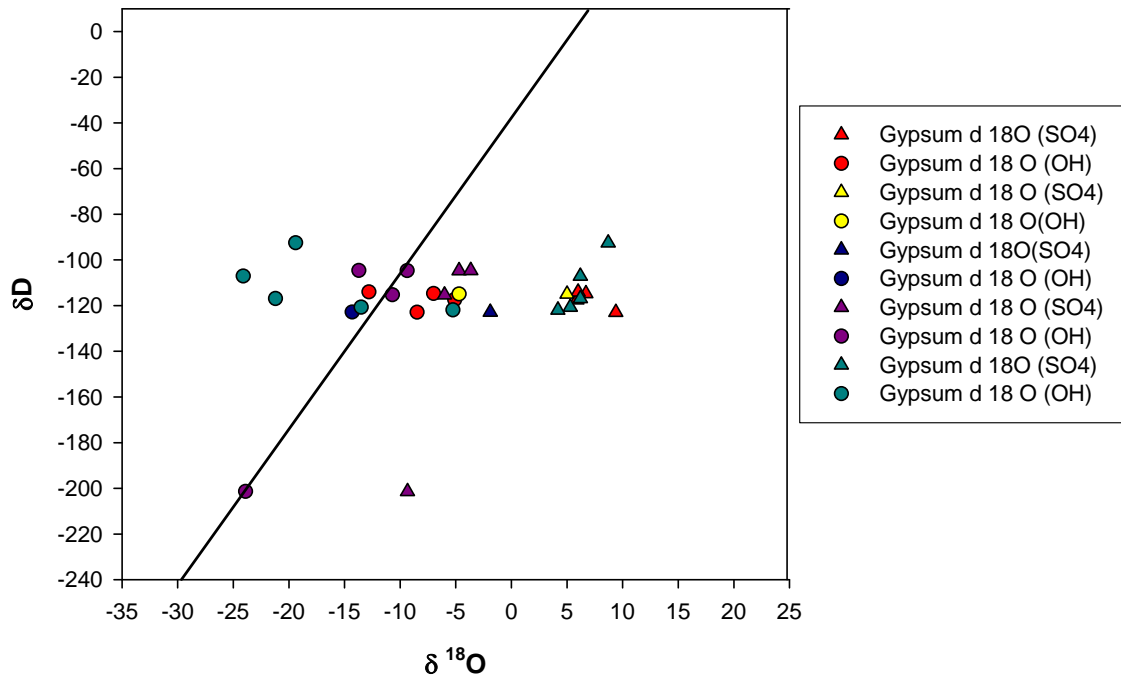
Figure 6. Graph of δ D vs. δ 18O of gypsum
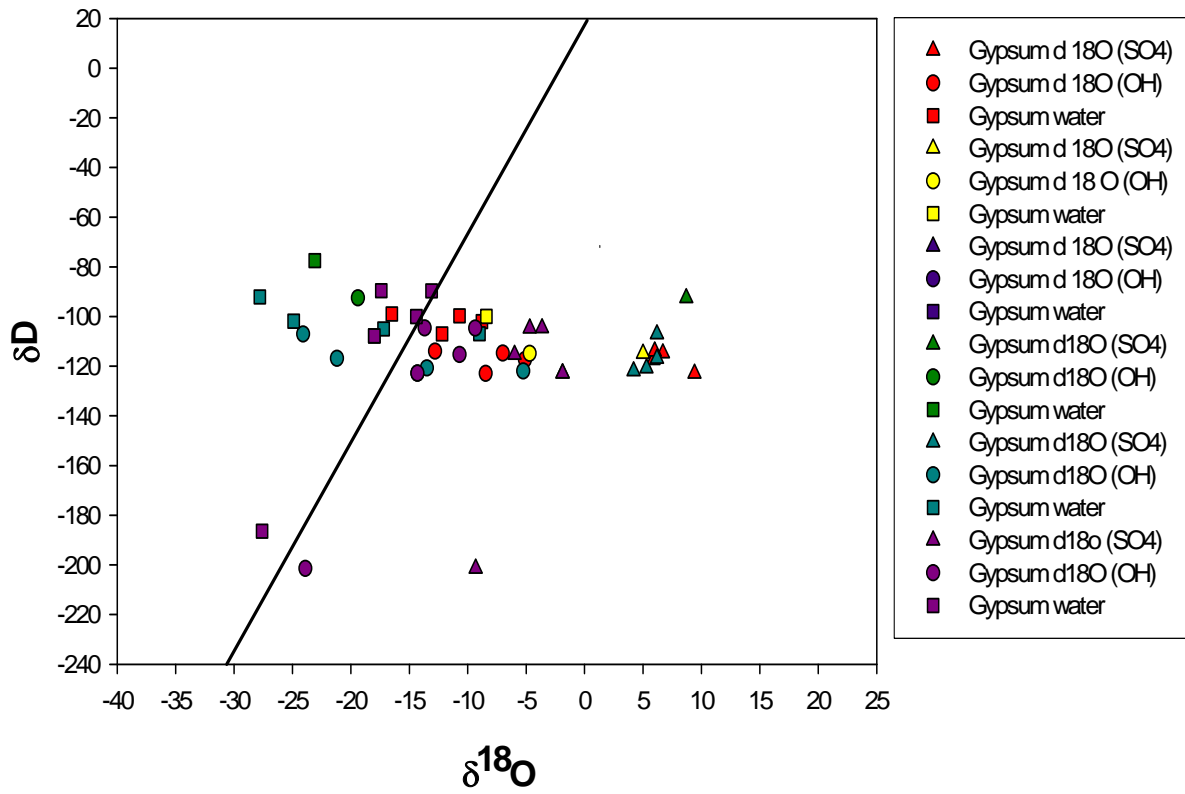
Figure 7. δD and δ^{18}O values of gypsum from different locations.
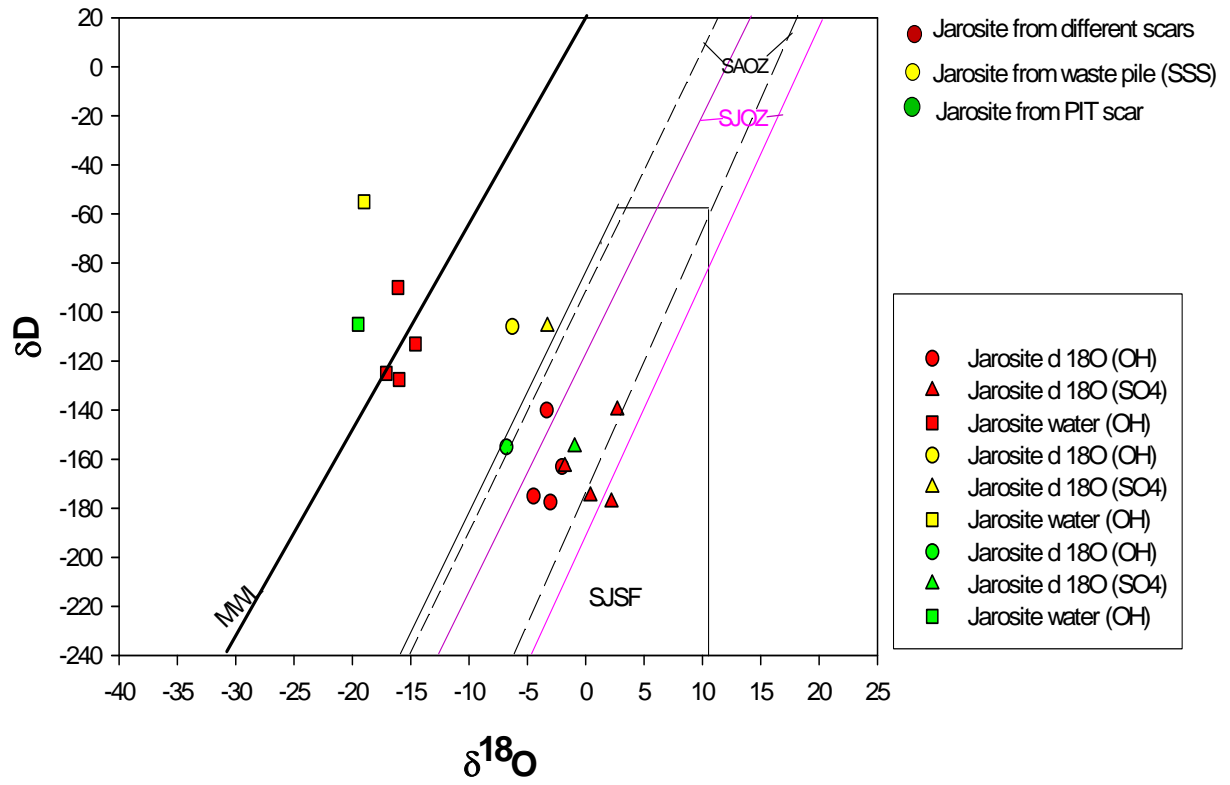
Figure 8. Graph showing δD and δ^{18}O values of jarosite from different locations.

10. Appendix

Appendix 1

Sample preparation

Mineralogical Separation: To separate kaolinite, clays and quartz from typical acid sulfate assemblages, mineral separation is essential. Kaolinite impurities are the most common in the case of alunite. They can be removed by several steps of centrifugation followed by ultrasonic suspension. If the amount of kaolinite is not very high in the samples, the dissolution in a dilute solution of HF is effective for removing most of the clay.

Chemical Separation (based upon the work of Rye, 1997):
- 60 mg sample + 125 mL 0.5N NaOH (ratio should be 1:2)
- Heating (at 80ºC) with continuous stirring for 3 hours, cover the beaker with watch glass to minimize the evaporation
- Filter with 1µ filter paper, make sure the filtrate is clear
- Heat the filtrate for a while till it reaches 80ºC
- Titrate it with 10N HCl solution till the pH reaches ~3
- Quickly add 2 mL of 0.5N $BaCl_2$ solution to the heated solution
- Observe the formation of white precipitate of $BaSO_4$
- Heat further with continuous stirring for 3 more hours
- Let it sit for overnight
- Filter the solution without stirring with 0.45µ filter paper
- Dry the white precipitate of $BaSO_4$ in the oven

Appendix 2

Sample size for different isotopic analysis

δD
Gypsum = 0.30 ± 0.1 mg
Jarosite = 0.35 ± 0.05 mg
Alunite = 0.35 ± 0.05 mg

$\delta^{34}S$
Gypsum = 1.5 ± 0.5 mg
Anhydrite = 0.5 ± 0.2 mg
Pyrite = 0.7 ± 0.2 mg
Jarosite = 2.5 ± 0.5 mg
Alunite = 2.5 ± 0.5 mg

$\delta^{18}O$ (bulk)
Gypsum = 0.22 ± 0.10 mg
Jarosite = 0.45 ± 0.10 mg
Alunite = 0.45 ± 0.10 mg

$\delta^{18}O$ (SO_4)

$BaSO_4 = 0.20 \pm 0.05$ mg

Standards and their isotopic values

For hydrogen	δD
Polyethylene IAEA CH 7	−100 ‰
HEKA Benzoic acid	−61.0 ‰

For oxygen	$\delta^{18}O$
HEKA Benzoic acid	25.1 ‰
NBS 127 $BaSO_4$	9.3 ‰

For sulfur	$\delta^{34}S$
NBS 127 $BaSO_4$	20.3 ‰
NBS 123 ZnS	17.3 ‰
NZ2 Ag_2S	21.0 ‰

Appendix 3

Fractionation equations for different minerals

Jarosite

$10^3 \ln \alpha$ (OH-H_2O) = 2.1 ($10^6/T^2$) – 8.77   calculated @ 40°C
$10^3 \ln \alpha$ (SO_4-H_2O) = 3.53 ($10^6/T^2$) – 6.91   calculated @ 40°C
$10^3 \ln \alpha$ (D-H_2O) = –50 ± 12 (250 to 450 °C)

Alunite

$10^3 \ln \alpha$ (OH-H_2O) = 2.28 ($10^6/T^2$) – 3.90   calculated @ 250°C
$10^3 \ln \alpha$ (SO_4-H_2O) = 3.09 ($10^6/T^2$) – 2.94   calculated @ 250°C
$10^3 \ln \alpha$ (D-H_2O) = –6 @ 250°C
                     –19 @ 450 °C

Gypsum

$10^3 \ln \alpha$ (SO_4-H_2O) = 3.7 (between 17 – 57 °C, independent of the temperature)
$10^3 \ln \alpha$ (D-H_2O) = –15 (between 17 – 57 °C, independent of the temperature)

4) Results

Sample ID	Mineral	$\delta^{18}O$ (bulk)
PIT VWL 0007 07	Jarosite	-3.264
SSS VWL 0001 07	Gypsum	1.208
SSS VWL 0002 07	Jarosite	-4.512
SSS VWL 0002 07	Gypsum	-6.072
SSS VWL 0003 07	Gypsum	-0.352
SSW VWL 0001 07	Gypsum	2.248
SSW VWL 0001 07	Gypsum dup	6.408
SSW VWL 0001 07 (unt)	Gypsum	5.562
SSW VWL 0002 07	Gypsum	-6.696
SSW VWL 0003 07	Gypsum	-7.424
SGS VWL 0001 07	Gypsum	-2.328
SGS VWL 0002 07	Gypsum	-13.664
SGS VWL 0003 07	Gypsum	-2.744
SGS VWL 0004 07	Gypsum	-2.016
SGS VWL 0005 07	Gypsum	0.896
SGS VWL 0005 07	Gypsum	-0.352
GMG PIT 0001 07	Gypsum	0.168
GMG pit 0001-07		-2.472
GMG pit 0001-07		-4.544
SCS VWL 0005 07	Gypsum	-5.552
SCS VWL 0005 07	Gypsum dup	-5.24
SCS VWL 0005 07 (unt)	Gypsum	-6.1
SCS VWL 0005 07 (unt)	Gypsum	-8.452
SCS VWL0005dup		-5.58
AR 163	Anhydrite	3.496
AR 89	Anhydrite	5.368
AR 165 (unt)	Anhydrite	6.444
AR 165	Anhydrite	8.28
AR-165	Gypsum	1.82
AR-165 dup	Gypsum	3.3
AR 140	Gypsum	1.624
AR-140	Gypsum	3.596
AR 86	Gypsum	0.168
AR 86 (unt)	Gypsum	0.564
AR-86	Gypsum	1.376
AR-23	Gypsum	4.04
AR-44	Gypsum	0.488
PIT VWL 0007 07	Jar(pink)	-1.496

Sample ID	Mineral	$\delta^{18}O\ (SO_4)$
AR 86 (t)	Gypsum	5.954
AR 44 (t)	Gypsum	7.032
AR 165 (t)	Gypsum	6.738
AR 140 (t)	Gypsum	5.856
AR 23 (t)	Gypsum	9.384
AR 136 (t)	Gypsum	7.424
AR 136 (t)	Gypsum dup	7.326
SSW VWL 0001 07 (t)	Gypsum	-7.57
SSW VWL 0002 07(t)	Gypsum	-3.65
SSW VWL 0003 07 (t)	Gypsum dup	-6.002
SSS VWL 0001 07 (t)	Gypsum	-5.806
SSS VWL 0002 07 (t)	Jarosite	-3.356
SSS VWL 0002 07 (t)	Jarosite dup	-3.16
SSS VWL 0002 07 (t)	Gypsum	-4.728
SSS VWL 0003 07(t)	Gypsum	5.268
SGS VWL 0001 07 (t)	Gypsum	4.19
SGS VWL 0002 07 (t)	Gypsum	-9.334
SGS VWL 0003 07 (t)	Gypsum	6.248
SGS VWL 0004 07 (t)	Gypsum	6.542
SGS VWL 0004 07 (t)	Gypsum	5.856
SGS VWL 0005 07 (t)	Gypsum	8.6588
SGS VWL 0005 07 (t)	Gypsum dup	8.6196
PIT VWL 0007 07 (t)	Jarosite (yellow)	-1.396
PIT VWL 0007 07 (t)	jarosite (yellow)dup	-0.514
GMG PIT 0001 07(t)	Gypsum	4.974
SCS VWL 0005 07 (t)	Gypsum	-1.886

Sample ID	Mineral	δD
PIT VWL 0007 07	Jarosite (Yellow)	-154.86
PIT VWL 0007 07	Jarosite dup	-154.99
PIT VWL 0007 07	Jarosite (yellow)	-144.442
SSS VWL 0001 07		-98.226
SSS VWL 0001 07	dup	-96.424
SSS VWL 0002 07	Jarosite	-111.96
SSS VWL 0002 07	Jarosite dup	-105.2
SSS VWL 0002 07	Jarosite	-106.494
SSS VWL 0002 07	Gypsum	-104.692
SSS VWL 0003 07		-120.698
AR 23	Gypsum	-122.88
AR 86		-112.112
AR 86		-115.716
AR 140		-117.412
AR 165		-114.126
AR 165		-115.186
SSW VWL 0001 07		-115.822
SSW VWL 0003 07	Gypsum	-115.292
SSW VWL 0002 07	Gypsum	-104.586
SGS VWL 0001 07	Gypsum	-121.864
SGS VWL 0002 07	Gypsum	-137.976
SGS VWL 0002 07	Gypsum dup	-177.62
SGS VWL 0002 07	Gypsum	-199.06
SGS VWL 0002 07	Gypsum dup	-203.74
SGS VWL 0003 07		-107.13
SGS VWL 0004 07		-116.882
SGS VWL 0005 07	Gypsum	-94.54
SGS VWL 0005 07	Gypsum dup	-90.38
GMG PIT 0001 07		-115.398
GMG PIT 0001 07		-114.338
SCS VWL 0005 07	Gypsum	-124.196
SCS VWL 0005 07		-121.334

Sample ID	Mineral	$\delta^{34}S$
SSS VWL 0001	Gypsum	1.93
SSS VWL 0002	Gypsum	2.6
SSS VWL 0002	Jarosite	2.16
SSSVWL 0003	Gypsum	11.2
SSW VWL 0001	Gypsum	1.29
SSW VWL 0002	Gypsum	2.45
SSW VWL 0003	Gypsum	2.15
PIT VWL 0007(j)	Jarosite dup (pink)	-6.7
PIT VWL 0007(j)	Jarosite dup (Yellow))	-6.5
SGS VWL 0001	Gypsum	10.8
SGS VWL 0002	Gypsum	0.9
SGS VWL 0003	Gypsum	8.74
SGS VWL 0004	Gypsum	9.9
SGS VWL 0004	Gypsum dup	10
SGS VWL 0005	Gypsum	8.81
SGS VWL 0004	Anhydrite	4.95
GMG PIT 0001-07	Gypsum	12.5
SCS VWL 0005	Gypsum	1.45
AR-23	Gypsum	12.6
AR-23	Gypsum	12.6
AR-23	Gypsum dup	12.6
AR-140	Gypsum	9.92
AR-140	Gypsum dup	9.61
AR-140	Gypsum	10.4
AR-44	Gypsum	6.17
AR-44	Gypsum	5.6
AR-44	Gypsum	6.36
AR-44	Gypsum dup	6.6
AR-165	Gypsum	9.44
AR-165	Gypsum dup	10.3
AR-86	Gypsum	7.44
AR-86	Gypsum dup	8.57
AR-136	Gypsum	9.36
AR-136	Gypsum	8.99
AR-136	Gypsum dup	9.27